Journal of Physics and Its Applications

Journal homepage : https://ejournal2.undip.ac.id/index.php/jpa/index

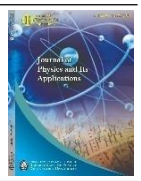

Analysis of Anthropogenic Seismic Noise Characteristics in Urban and Rural Areas of Bali Island Indonesia

Urip Setiyono[1,2], Mohammad Syamsu Rosid[1*], Prawito Prajitno[1], Supriyanto Rohadi[2], and Ade Andika Saputra[2]

[1]*Department of Physics, Faculty of Mathematics and Natural Sciences, Universitas Indonesia, Depok, Indonesia*
[2]*Meteorology, Climatology and Geophysics Agency (BMKG), Central Jakarta, Indonesia*

**Corresponding author: syamsu.rosid@ui.ac.id*

ARTICLE INFO

Article history:
Received: 2 October 2026
Accepted: 21 February 2026
Available online: 30 May 2026

Keywords:
Anthropogenic noise
Power Spectral Density (PSD)
Tourist season
Site characterization
Bali, Indonesia

ABSTRACT

Seismic noise significantly affects the quality of earthquake detection data. This study analyzes the characteristics of anthropogenic seismic noise recorded at eight permanent broadband seismic stations in the urban and rural areas of Bali, Indonesia, from 2020 to 2024. Power spectral density (PSD) was analyzed in the 1–10 Hz band, which primarily reflects human activity. Seasonal variability was evaluated by comparing the low tourism period (March) with the peak season (August). Urban stations generally show dominant frequencies in the mid- to high-frequency range (~4–8 Hz), together with seasonal ΔPSD increases of up to ~6 dB, and frequent exceedance of the New High Noise Model (NHNM). In contrast, stations in rural areas recorded lower dominant frequencies (~1–2,5 Hz) with moderate variations and, in some cases exhibited negative ΔPSD. Local geological factors played a significant role: volcanic breccias and massive lava flows dampened high-frequency noise, while loose sediments amplified anthropogenic signals. Anomalies during specific periods, when community mobility is drastically reduced, highlight the sensitivity of rural stations to changes in human activity intensity. These results provide a station-scale framework for diagnosing anthropogenic seismic noise and establish a baseline for improving seismic data quality and supporting seismic network design in densely populated and tourism-driven region.

1. Introduction

Human activities in densely populated areas or economic centers can generate continuous vibrations recorded using seismic monitoring instruments, such as seismographs. This phenomenon, known as seismic noise, encompasses non-earthquake vibration signals originating from both natural sources [1] and anthropogenic sources [2–4]. In seismic observation practice, anthropogenic noise generated by traffic, industry, construction, and tourism often reduces the signal-to-noise ratio (SNR) and obscures the detection of significant seismic events [5, 6]. Spectrally, anthropogenic noise typically emerges within the mid- to high-frequency range and exhibits temporal patterns that are closely correlated with the intensity of human activities [7].

Bali Island provides a unique natural context for examining the dynamics of anthropogenic seismic noise due to its status as one of the world's major tourist destinations [8], with pronounced fluctuations in human activity intensity driven by seasonal tourism cycles. This contrast is particularly evident between urban areas, which are dense with transportation, commercial, and entertainment activities, and rural areas, which remain relatively quiet. Although several previous studies have documented reductions in seismic noise during the COVID-19 pandemic [9, 10, 5], investigations into regular seasonal variations recurring annually, especially in regions with tourism dynamics as intense as Bali, remain very limited.

Several studies have demonstrated a strong correlation between human activities and the intensity of seismic noise, even at highly specific temporal resolutions, such as daily variations or activity-specific patterns [11–14]. However, distinguishing the spectral signatures of different noise sources, such as traffic, construction, and industry, remains challenging due to frequency overlaps and pronounced temporal variability [15–17]. This complexity is particularly relevant in the context of Bali, where the interplay between tourism-related and non-tourism factors, such as local geology, topography, and environmental conditions, may influence the characteristics of the recorded seismic noise.

This study characterizes anthropogenic seismic noise in Bali by leveraging spatial (urban vs. rural) and temporal (high vs. low tourism season) variations. The objectives are to identify dominant frequencies associated with human activities, quantify seasonal dynamics of ΔPSD, and evaluate the influence of local geology on noise propagation based on five years of continuous multi-station observations (2020–2024). Unlike many previously studied tourist regions, Bali integrates strong tourism-driven seasonality, compact urban–rural–

coastal gradients, and pronounced geological heterogeneity within a limited island-scale setting, enabling anthropogenic seismic noise to be evaluated under spatially consistent tectonic and climatic conditions.

Within this framework, Bali is positioned not merely as a local case study but as a natural laboratory to investigate the complex interplay between human activities and seismic noise, with broader implications for site evaluation and seismic network design in tourist destinations and other major centers of human activity worldwide. This framework further establishes a foundation for continuous seasonal monitoring and site-response characterization aimed at refining station-specific noise diagnostics and strengthening seismic data quality in complex human-environment settings.

2. Method

2.1. Data

This study uses three-component seismic waveform data in .mseed format recorded by eight permanent broadband stations across Bali, Indonesia, accessible via https://geof.bmkg.go.id/. The stations are classified according to their surrounding environments into three categories: urban (Denpasar/DNP, Kintamani/KBBI, Badung/BDBI, Seririt/SBBM), semi-urban (Negara/NJBM), and rural (Singaraja/SRBI, Nusa Penida/NKBI, Rangdo/RTBI). The spatial distribution of the stations and administrative boundaries of Bali is shown in Fig. 1. Administrative boundary data were obtained from the Indonesian Geospatial Agency, with base layers sourced from OpenStreetMap, and all maps were prepared using QGIS version 3.22. The distribution of these stations corresponds to variations in anthropogenic activity, which are strongly influenced by the intensity of tourist visits across different regencies and municipalities. This spatial arrangement allows for comparative analyses of seismic noise patterns in areas with distinct levels of tourism-related human activity.

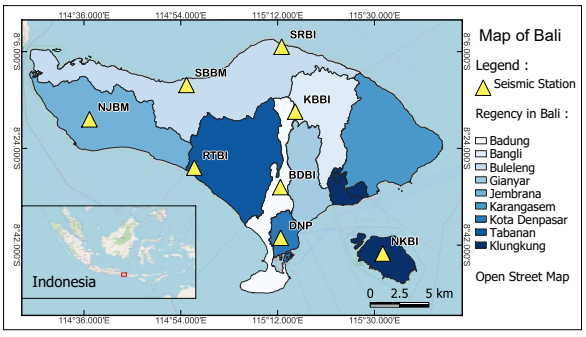

Fig. 1: Locations of eight broadband seismic stations in Bali. Inset shows the regional setting of Bali within Indonesia.

The seismic waveform data used in this study were collected in March and August, representing the low and high tourism seasons in Bali, respectively [18]. The analysis covers a five-year period (2020–2024) to ensure robustness across interannual variability, including the COVID-19 period. For each selected month, 6–10 representative days were chosen, spanning the beginning, middle, and end of the month to capture intra-month variability while minimizing the influence of short-term anomalies. Tourist arrival data for March and August over the same period (Fig. 2) were obtained from the Provincial and Regency/Municipality Tourism Offices in Bali, demonstrating a consistent pattern in which March corresponds to seasonal minima and August to seasonal maxima in tourist activity across years and administrative regions. Accordingly, the March–August comparison is intended to capture relative seasonal contrasts in anthropogenic activity rather than absolute activity levels.

In addition to the administrative map and station locations, the distribution of potential anthropogenic noise sources surrounding each station was analyzed with respect to their relative direction and distance. The rose diagrams in Fig. 3 illustrates the concentration of sources within radii of <1 km, 1–5 km, 5–10 km, and >10 km. These sources include tourist attractions, schools, offices, main roads, airports, ports, industrial zones, and densely populated residential areas. Each category was mapped according to its orientation and proximity to provide spatial context for the recorded noise characteristics.

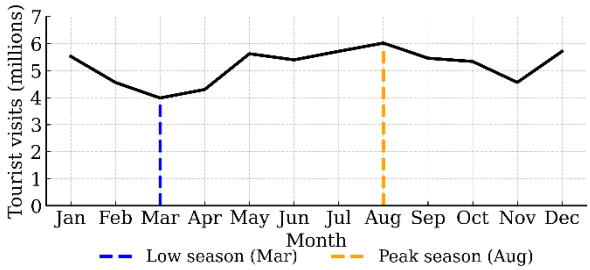

Fig. 2: Total monthly tourist arrivals in Bali aggregated for 2020–2024, highlighting March (low season) and August (peak season).

2.2. Methodology

The characterization of seismic noise was carried out through a spectrophotometer.

- Power Spectral Density Analysis:

Daily waveform data from each station were processed using the Welch method with fixed Hanning-tapered windows and 50% overlap [19, 20]. PSD was calculated for March and August of each year to represent seasons of low and high anthropogenic activity and subsequently compared with the New Low Noise Model (NLNM) and New High Noise Model (NHNM) [21]. The spectral curves, plotted over the 0.001–10 Hz range with PSD expressed in dB (Fig. 4), were then classified according to [22] and [6] into three categories: short-period noise (0.1–1 s), ocean microseisms (1–20 s), and long-period noise (20–900 s) to identify the characteristics of local seismic noise.

- Dominant Frequency Extraction:

Dominant anthropogenic frequencies were extracted using short-time Fourier transforms of band-pass filtered waveforms (1–10 Hz), selecting the frequency of maximum spectral amplitude in each sliding window as the dominant frequency, representing human-activity-related seismic sources [23, 24]. Daily median values were aggregated into monthly means and visualized to assess seasonal and interannual variability. Those reflects source-related

anthropogenic activity and is distinct from the site fundamental frequency (f_0) derived from HVSR analysis.

- Seasonal Comparison Analysis (ΔPSD):

ΔPSD values were calculated as the difference between the average PSD in August and March at each station for each year. These values were then graphically visualized to identify years with significant fluctuations and anomalies (e.g., negative ΔPSD values).

- Integration with Local Geological Data:

The station locations were mapped against the geological map of Bali to assess the influence of lithology and local morphology on variations in dominant frequency and noise amplitude. Geological zonation based on rock age and lithology type (tertiary, quaternary, volcanic, and sedimentary) was employed as spatial context in interpreting the results.

- Spatial Analysis Based on Urban–Rural Zoning:

All PSD, dominant frequency, and ΔPSD results were analyzed across urban–rural zones to evaluate the spatial gradient of anthropogenic noise. The stations were grouped according to their urban–rural classification.

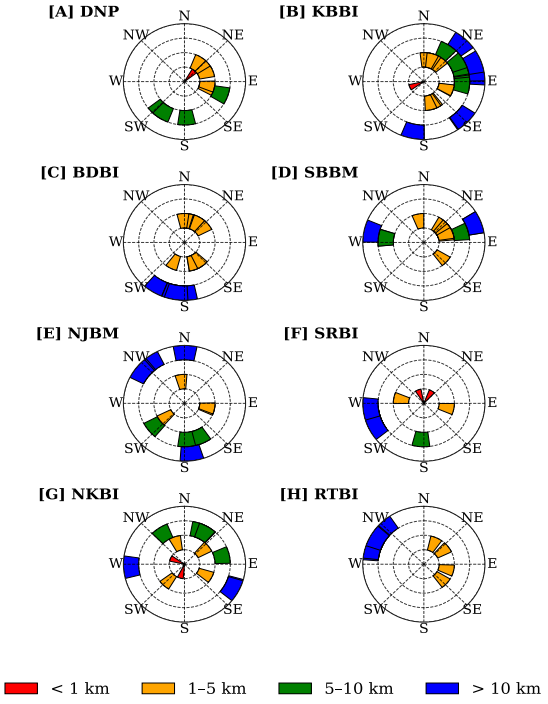

Fig. 3: Rose diagrams showing distance–azimuth distributions of potential anthropogenic noise sources around eight seismic stations in Bali.

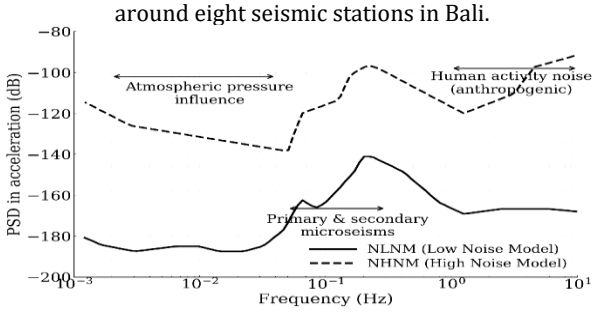

Fig. 4: Reference seismic ambient noise levels based on the Peterson (1993) model across different frequency bands. Modified from [22].

2.3. Validation and Limitations

This approach has several advantages and limitations. The selection of representative days (6–10 days per month) reduces the computational load in seasonal analyses; however, the full range of intra-month variability is not fully captured. The analysis is focused on two key months (March and August), representing the annual tourism cycle; therefore, long-term changes outside this period are not the primary focus. Nevertheless, this strategy is well-suited to highlighting regular seasonal contrasts while minimizing bias arising from seismotectonic events or temporary non-tourism-related occurrences.

3. Result and Discussion

Analysis of the average power spectral density (PSD) in the 1–10 Hz range reveals a clear contrast between urban and rural stations in Bali (Fig. 5). Urban sites (DNP, KBBI, BDBI, and SBBM) consistently record higher PSD values, particularly at frequencies above 5 Hz, and often exceed the New High Noise Model (NHNM). Elevated PSD levels at urban stations are primarily attributed to the intense human activities occurring nearby, including traffic, industry, and tourism.

Table 1: Seismic noise characteristics of urban and rural stations in Bali 2020-2024.

Station	ΔPSD Range (dB)	Key Notes
DNP	–1.52–+1.74	Highest absolute noise levels; consistently above NHNM; negative anomaly in 2021 linked to non-tourism activities
KBBI	+2.48 – +3.15	ΔPSD consistently positive; strong seasonal response to tourism; PSD frequently above NHNM during peak season
BDBI	+2.75 – +4.03	Clear sensitivity to tourist mobility; PSD often near or above NHNM
SBBM	+3.86 – +5.68	Strongest seasonal responsiveness, but absolute PSD remains below NHNM due to massive lava lithology
NJBM	+1.54 – +2.38	Moderate seasonal increase; transitional pattern between rural and urban sites
SRBI	+1.65 – +5.79	Major surge in 2021 (>+5 dB) during COVID-19 restrictions; strong seasonal variability
NKBI	–0.27 – +5.72	Large seasonal surges in 2021–2023; negative anomaly in 2024 linked to maritime activity
RTBI	–0.29 – +3.09	Lowest and most stable PSD; consistently below NHNM; negative anomaly in 2020 influenced by microseisms.

In addition, differences in dominant frequency provide further insights. Noise at higher frequencies

(>5 Hz) tends to originate from shallower and near-surface sources. This reflects not only the quantity of activity (the number of human activities) but also the quality of those activities, namely their increasing dynamism, progressiveness, and intensity. In other words, the prevalence of higher-frequency patterns in urban areas indicates more intense and diverse surface-level human activities compared to rural areas.

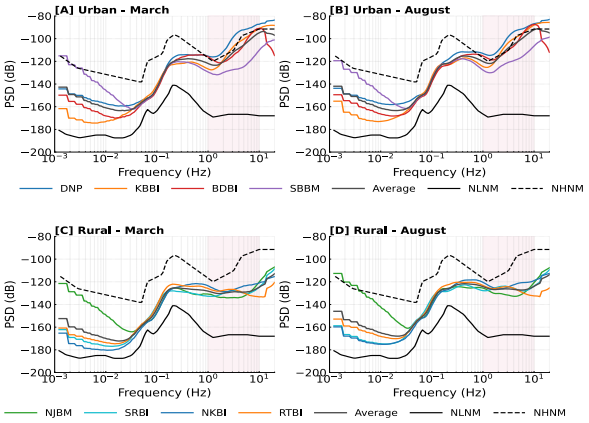

Fig. 5: Average PSD curves at urban and rural stations in Bali during March and August (2020–2024): (A) urban–March, (B) urban–August, (C) rural–March, and (D) rural–August.

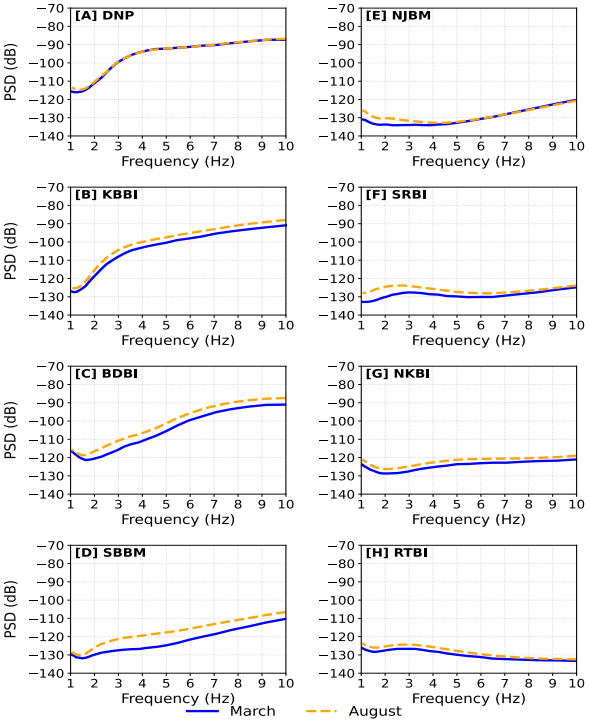

Fig. 6: Average PSD in the 1–10 Hz frequency band at eight seismic stations in Bali during March and August (2020–2024): (A) DNP, (B) KBBI, (C) BDBI, (D) SBBM, (E) NJBM, (F) SRBI, (G) NKBI, and (H) RTBI.

Seasonal differences are clearly observed, with the August curves shifted upward compared to March (Fig. 6), resulting in ΔPSD values ranging from +1.20 to +5.68 dB (Fig. 7). The DNP station exhibits the highest absolute noise levels with limited seasonal variation (<+2 dB), whereas SBBM displays the strongest seasonal response (+5.68 dB in 2023). In contrast, rural stations (NJBM, SRBI, NKBI, and RTBI) generally remain closer to the New Low Noise Model (NLNM), although SRBI and NKBI recorded significant spikes in 2021 (>+5 dB), and occasional negative ΔPSD anomalies were observed (RTBI in 2020; NKBI in 2024; DNP in 2021).

Overall, the results highlight three main patterns: (1) higher baseline noise levels in urban areas due to the massive quantity of human activities, (2) stronger seasonal variability in urban zones compared to rural ones, and (3) local anomalies at rural stations. These findings indicate that the interpretation of PSD should consider the magnitude of values (quantitative) and frequency distribution, which reflects the quality and intensity of human activities (Table 1).

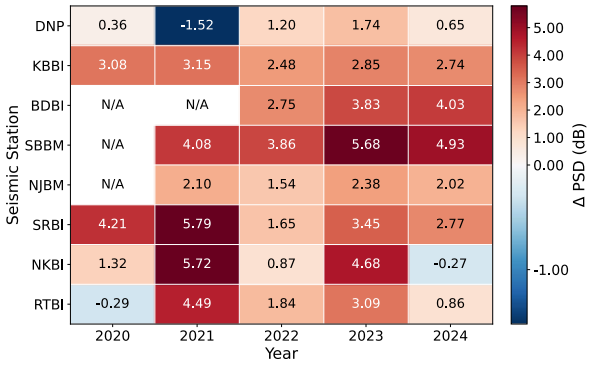

Fig. 7: Seasonal differences in anthropogenic seismic noise (ΔPSD = August − March) in the 1–10 Hz band at eight stations in Bali for 2020–2024. "N/A" indicates years with unavailable data.

Table 2: Monthly tourist arrivals (March = M, August = A) for seismic stations in Bali (2020–2024).

Station	2020	2021	2022	2023	2024
DNP-M	61.332	39.374	96.977	184.889	239.192
DNP-A	16.644	13.480	185.223	200.519	218.808
KBBI-M	-	8.737	46.414	100.790	71.995
KBBI-A	-	0	110.314	148.466	119.963
BDBI-M	167.842	2	15.603	377.510	480.819
BDBI-A	175	23	283.239	533.839	631.468
SBBM-M	24.530	24.567	67.455	82.073	86.561
SBBM-A	24.954	1.874	139.580	146.567	200.771
NJBM-M	7.101	12.761	17.551	21.903	20.295
NJBM-A	6.400	1.521	15.273	23.125	22.419
SRBI-M	24.530	24.567	67.455	82.073	86.561
SRBI-A	24.954	1.874	139.580	146.567	200.771
NKBI-M	13.542	72	194	37.893	73.197
NKBI-A	89	12	47.836	77.147	144.626
RTBI-M	140.988	45.064	76.631	226.946	170.167
RTBI-A	92.260	0	195.490	343.255	319.752

To support the interpretation of seasonal ΔPSD in Fig. 7, Table 2 presents the monthly number of tourist arrivals in March and August (2020–2024). August generally coincides with the peak tourism season, whereas March is typically lower, with anomalies in 2020–2021 due to COVID-19 restrictions. The data represent total tourist arrivals at the regency/city level and are therefore not limited to the immediate surroundings of the seismic stations. This comparison helps assess whether variations in seismic noise are more strongly influenced by tourism intensity or other local factors.

Seasonal and interannual variability further reinforce the differences between the two zones. Urban stations consistently exhibit increased PSD during peak tourism seasons, with DNP maintaining

the highest amplitudes, while KBBI and BDBI record sharp seasonal rises associated with human mobility. At SBBM, values remain below the NHNM but display moderate seasonal increases (Fig. 8). This condition can be explained by massive lava lithology (Tpva), which acts as a natural low-pass filter, thereby attenuating the high-frequency noise that typically dominates urban locations [25]. This phenomenon underscores that urban sites are not always characterized by elevated noise levels but are strongly influenced by local geological conditions.

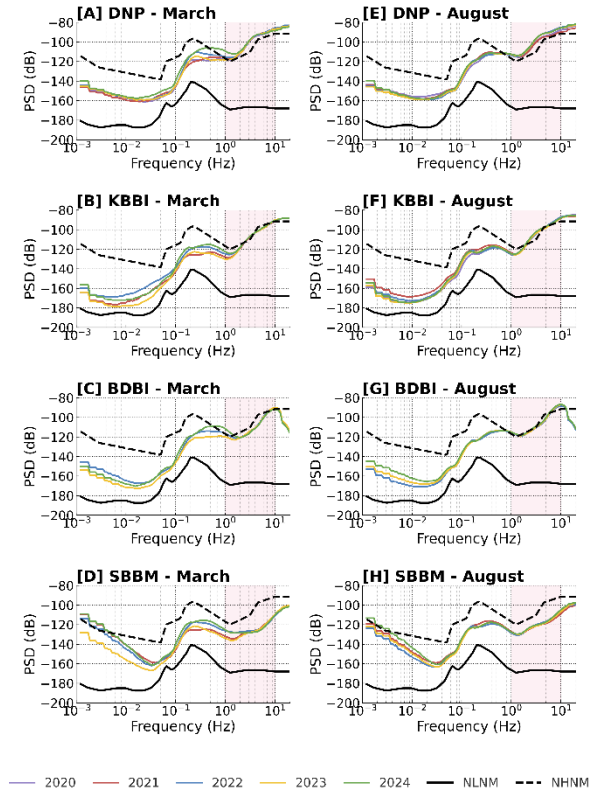

Fig. 8: Average PSD at four urban stations in Bali during March and August (2020–2024): (A) DNP–March, (B) KBBI–March, (C) BDBI–March, (D) SBBM–March, (E) DNP–August, (F) KBBI–August, (G) BDBI–August, and (H) SBBM–August. The 1–10 Hz frequency band is highlighted.

Rural stations (Fig. 9) consistently remain below the NHNM throughout all years, with RTBI recording the lowest and most stable amplitudes in the 1–4 Hz range. The massive lava lithology of Jembrana, which effectively attenuates noise, combined with its distance from major tourism centers, provides the primary explanation for the low noise levels at RTBI. In contrast, NKBI and SRBI exhibited substantial spikes in 2021 with ΔPSD values exceeding +5 dB. This phenomenon coincided with COVID-19 restrictions, when the March baseline was exceptionally low, making the relative difference with August appear extreme. Thus, rural sites are more sensitive in detecting extreme changes in human mobility, whereas urban sites tend to be more stable due to the persistent influence of permanent anthropogenic sources [26].

To quantitatively assess the extent to which urban and rural stations exceed the New High Noise Model (NHNM), the average PSD curves are shown in Figs. 8 and 9 complement exceedance-based metrics summarized in Table 3. Specifically, the percentage of PSD estimates within the 1–10 Hz anthropogenic frequency band that exceeds the NHNM threshold was computed, together with a spectral proximity measure (NHNM–PSD) that captures how close the spectra remain to the NHNM even when exceedance does not occur.

This combined approach allows urban–rural contrasts to be evaluated beyond visual inspection of mean spectra, addressing both the frequency of exceedance and near-threshold behavior across seasons.

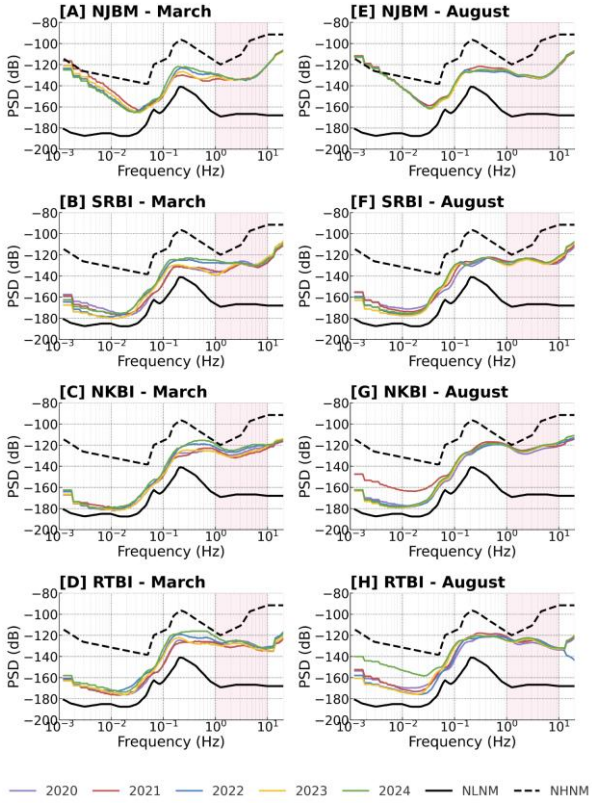

Fig. 9: Average PSD at four rural stations in Bali during March and August (2020–2024): (A) NJBM–March, (B) SRBI–March, (C) NKBI–March, (D) RTBI–March, (E) NJBM–August, (F) SRBI–August, (G) NKBI–August, and (H) RTBI–August. The 1–10 Hz frequency band is highlighted.

Table 3 reveals a clear quantitative contrast between urban and rural stations in terms of NHNM exceedance within the 1–10 Hz band. DNP exhibits persistent exceedance, reaching 98.5% in March and 100% in August, while KBBI and BDBI show moderate exceedance that increases seasonally (23.7%–58.5% and 21.0%–43.2%, respectively). In contrast, all rural stations (NJBM, NKBI, RTBI, and SRBI) consistently remain below the NHNM threshold across both seasons (0% exceedance), as reflected by positive spectral proximity values. Notably, SBBM, despite its urban setting, also remains systematically below the NHNM (0% exceedance), indicating that local site conditions can effectively suppress high-frequency anthropogenic noise even during peak tourism periods. These results demonstrate that while seasonal human activity strongly modulates high-frequency noise levels, NHNM exceedance is not an inherent characteristic of urban environments but reflects the combined effects of source intensity, site conditions, and local geology.

The dominant frequency patterns shown in Fig. 10 highlight a clear contrast between urban and rural seismic environments in Bali. Urban stations consistently exhibit dominant frequencies in the mid- to high-frequency range, generally between ~5 and 9

Hz, with several years approaching the upper bound of the analyzed band. This behavior is observed persistently at stations such as KBBI and BDBI in both March and August, indicating stable high-frequency dominance that is largely insensitive to seasonal changes. DNP remains comparatively stable around ~4 Hz across years, whereas SBBM shows lower and more variable dominant frequencies (approximately ~1.5–4.5 Hz). In comparison, most rural stations cluster at low dominant frequencies, with NJBM, NKBI, and RTBI consistently remaining near ~1.1–1.7 Hz across both seasons. Within the rural group, SRBI stands out by repeatedly reaching the highest dominant frequencies (roughly ~1.5–2.5 Hz in March and ~1.9–2.2 Hz in August), suggesting a site-specific elevation relative to other rural stations. Overall, the heatmaps indicate that dominant-frequency behavior varies markedly by station and is not fully captured by a simple urban–rural label alone. This observation points to the influence of localized conditions—such as nearby human activity or site-specific environmental factors—superimposed on the broader rural background [26].

Table 3: Aggregated NHNM exceedance (1–10 Hz) and spectral proximity for seismic stations in Bali (2020–2024)

Station	March NHNM exceedance (%)	August NHNM exceedance (%)	Closeness to NHNM (dB)–March	Closeness to NHNM (dB)–August
DNP	98.5	100.0	−11.2	−11.6
KBBI	23.7	58.5	−2.9	−6.2
BDBI	21.0	43.2	−1.6	−4.4
SBBM	0.0	0.0	+8.6	+9.6
NJBM	0.0	0.0	+12.0	+7.6
NKBI	0.0	0.0	+5.5	+3.3
RTBI	0.0	0.0	+8.0	+5.5
SRBI	0.0	0.0	+8.9	+7.4

The spatial analysis of eight permanent seismic stations in Bali reveals that variations in seismic noise within the 1–10 Hz frequency range are closely linked to local geological conditions and the level of anthropogenic activity surrounding each site. In general, stations located on young volcanic formations dominated by tuff, lahar, volcanic breccia, and pumiceous deposits (e.g., Qpbb and Tpva), as well as unconsolidated sedimentary units such as conglomerate and sandstone (QTsp), exhibit distinct spectral responses compared to those situated on more compact carbonate or massive volcanic rocks (e.g., Tmps and Qpvj).

The spatial distribution of dominant frequencies derived from PSD analysis reveals a clear contrast between urban and rural stations (Fig. 11). In the urban group, KBBI and BDBI—both located on the Buyan–Bratan Group and Batur volcanics (Qpbb)—consistently show dominant frequencies in the mid- to high-frequency range (~5–8 Hz), particularly during August. DNP, which is also situated on Qpbb, generally exhibits moderate dominant frequencies (~4–5 Hz). The Qpbb unit is dominated by volcanic deposits, mainly tuff and lahar, whose heterogeneous layering and variable compaction can enhance site amplification in the mid- to high-frequency bands [25].

In contrast, SBBM, located on the Asah Formation (Tpva), displays a mixed spectral response, alternating between low (~1–3 Hz) and moderate (~3–5 Hz) dominant frequencies across years. The Tpva unit is characterized by lava, volcanic breccia, and pumiceous tuff, locally intercalated with calcareous sediments. Such stiffer near-surface materials may attenuate high-frequency energy, while internal heterogeneity and interbedded layers can still promote localized resonance [27–29].

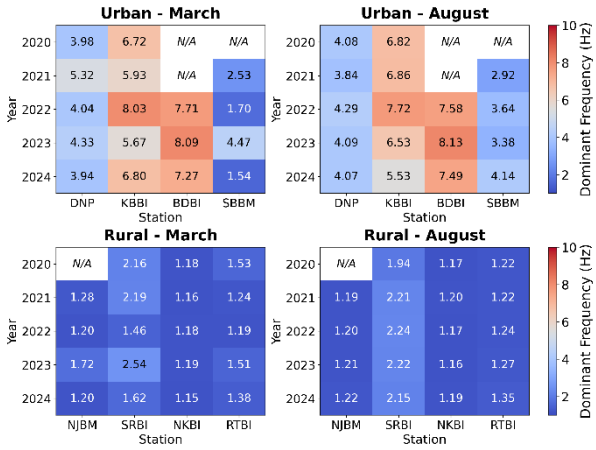

Fig. 10: Heatmap of dominant frequencies (1–10 Hz) derived from monthly average PSD at urban and rural seismic stations in Bali during March and August (2020–2024). "N/A" indicates years with unavailable data.

Rural stations are predominantly characterized by low dominant frequencies. RTBI, located on the Jembrana volcanics (Qpvj; lava, volcanic breccia, and tuff), consistently shows low-to-moderate dominant frequencies (~1–2 Hz), suggesting reduced anthropogenic forcing and stronger control by background ambient noise. NKBI, situated on the Southern Formation (Tmps), also exhibits low dominant frequencies (~1–1.2 Hz) across years. In contrast, SRBI—located on Tpva—shows relatively elevated dominant frequencies (~2–2.5 Hz) compared with RTBI and NKBI, consistent with the stiffer lava–breccia-dominated setting of the Asah Formation while still allowing localized resonance due to lithological heterogeneity [28–30]. NJBM, situated on the Palasari Formation (QTsp; conglomerate, sandstone, and reef limestone), likewise displays dominant frequencies in the low-frequency range (~1–2 Hz), consistent with rural background conditions. The presence of conglomerate and sandstone sediments may facilitate the amplification of anthropogenic waves.

Importantly, these PSD-derived dominant frequencies reflect temporally varying external forcing (anthropogenic and environmental sources), whereas HVSR-derived fundamental frequencies (f_0) represent intrinsic site resonance controlled by shallow geological structure. The systematic variation of f_0 across stations, from low values (~1.5–2.3 Hz) to higher values (>4 Hz), supports the interpretation that near-surface lithology and compaction govern resonance characteristics, while PSD-dominant frequencies capture the prevailing noise sources at each site. Such externally driven spectral variability is consistent with previous studies demonstrating how anthropogenic vibrations propagate through near-surface sediments and

transportation corridors, modulating local noise characteristics [30–32].

Overall, the observed patterns highlight the combined influence of lithology, rock compaction, and proximity to anthropogenic sources in shaping seismic noise characteristics [34–37]. These results underscore the importance of considering local geology in seismic noise interpretation [38] and station placement strategies [39].

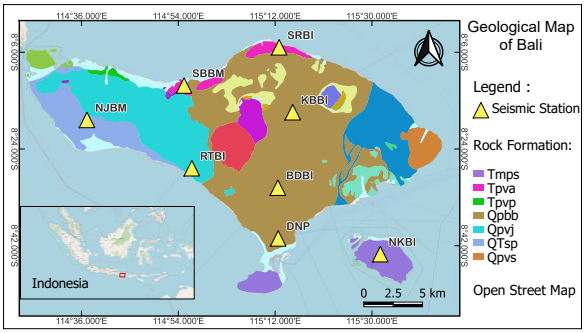

Fig. 11: Geological map of Bali showing the locations of seismic stations and major lithological units [33]. Inset shows the regional setting of Bali within Indonesia and base layers from OpenStreetMap.

Seasonal anomalies further highlight the sensitivity to changes in human mobility. SRBI and NKBI recorded sharp frequency drops (down to ~1–3 Hz) during 2020–2021, coinciding with COVID-19 restrictions, with ΔPSD exceeding +5 dB. Negative ΔPSD anomalies at DNP (2021), RTBI (2020), and NKBI (2024) indicate that non-tourism factors such as local traffic, religious activities, or ocean microseisms may become more dominant than tourism-related activities.

Overall, the findings demonstrate that administrative urban–rural classification alone is insufficient for evaluating seismic station sites. Instead, it must be integrated with anthropogenic activities, geological conditions, and seasonal dynamics. Rural stations function as highly sensitive indicators of changes in human mobility, whereas urban stations consistently record high and persistent levels of anthropogenic noise driven by daily human activities. Bali, with its distinctive tourism cycles, serves as a natural laboratory for investigating the interactions between human activities and seismic noise, providing valuable insights for earthquake monitoring network design and site evaluation in regions with intensive tourism or high population density.

4. Conclusion

This study reveals a clear contrast between seismic stations located in urban and rural areas of Bali. Urban stations consistently exhibit elevated dominant frequencies and positive ΔPSD values, consistent with persistent anthropogenic activity throughout the year. In contrast, rural stations show lower dominant frequencies and smaller baseline ΔPSD values yet display stronger relative spectral responses to extreme mobility changes, such as during the COVID-19 pandemic and periods of activity restrictions.

Negative ΔPSD anomalies at several stations confirm that seismic noise in Bali is not solely influenced by tourism intensity but results from multiple interacting processes involving non-tourism local activities and cultural factors. Furthermore, geology is demonstrated to be a primary controlling factor: unconsolidated volcanic lithologies amplify high-frequency noise, whereas massive rocks and compact carbonates act as natural filters that attenuate noise propagation, even at urban sites.

Based on these results, three key conclusions can be drawn. First, anthropogenic seismic noise in Bali exhibits a systematic urban–rural contrast, with urban stations showing persistently elevated PSD levels and rural sites displaying larger relative ΔPSD excursions. Second, local lithology strongly modulates high-frequency noise propagation, with unconsolidated volcanic and sedimentary units amplifying anthropogenic signals, while massive volcanic and carbonate rocks act as natural filters. Third, rural stations exhibit higher relative sensitivity to mobility changes because of their low baseline noise. These results provide quantitative guidance for seismic station site evaluation and network design in densely populated and tourism-driven regions.

Acknowledgment

We gratefully acknowledge the Indonesian Agency for Meteorology, Climatology, and Geophysics (BMKG) for financial support of scholarship, for providing the seismic data, and for granting permission to use these data in this publication. We thank Arya Bani Pangestu, Dwi Karyadi, and Nova Heryandoko for their technical assistance and constructive discussions. We also acknowledge the Tourism Offices of the regencies and municipalities in Bali Province and the valuable input from colleagues during manuscript preparation.

References

[1] C. Rossi, F. Grigoli, P. Gasperini, S. Gandolfi, C. Cocorullo, T. Gukov, and P. Macini, "Seismic Noise Reduction as a Function of Depth Recorded by a Vertical Array Installed in a 285-m-Deep Borehole at a Gas Storage Field in Northern Italy," Seismol. Res. Lett. 94(4), 1925–1935 (2023).

[2] A. Pakhomov and T. Goldburt, "Seismic signals and noise assessment for foot step detection range estimation in different environments," Proc. SPIE - Int. Soc. Opt. Eng. 5417, 87–98 (2004).

[3] J. R. R. Ritter and H. Sudhaus, "Characterization of small local noise sources with array seismology," Near Surf. Geophys. 5(4), 253–261 (2007).

[4] Y. Yang and F. Niu, "Using unsupervised machine learning for clustering seismic noise: a case study of a dense seismic array at the Weifang segment of the Tanlu Fault," Acta Geophys. Sin. 65(7), 2573–2594 (2022).

[5] T. Lecocq, S. P. Hicks, K. van Noten, K. van Wijk, P. Koelemeijer, R. S. M. de Plaen, F. Massin, G. Hillers, R. E. Anthony, M.-T. Apoloner, M. Arroyo-Solórzano, J. D. Assink, P. Büyükakpınar, A. Cannata, F. Cannavo, S. Carrasco, C. Caudron, E. J. Chaves, D. G. Cornwell, D. Craig, O. F. C. den Ouden, J. Diaz, S. Donner, C. P. Evangelidis, L. Evers, B. Fauville, G. A. Fernandez, D. Giannopoulos, S. J.

Gibbons, T. Girona, B. Grecu, M. Grunberg, G. Hetényi, A. Horleston, A. Inza, J. C. E. Irving, M. Jamalreyhani, A. Kafka, M. R. Koymans, C. R. Labedz, E. Larose, N. J. Lindsey, M. McKinnon, T. Megies, M. S. Miller, W. Minarik, L. Moresi, V. H. Márquez-Ramírez, M. Möllhoff, I. M. Nesbitt, S. Niyogi, J. Ojeda, A. Oth, S. Proud, J. Pulli, L. Retailleau, A. E. Rintamäki, C. Satriano, M. K. Savage, S. Shani-Kadmiel, R. Sleeman, E. Sokos, K. Stammler, A. E. Stott, S. Subedi, M. B. Sørensen, T. Taira, M. Tapia, F. Turhan, B. van der Pluijm, M. Vanstone, J. Vergne, T. A. T. Vuorinen, T. Warren, J. Wassermann, and H. Xiao, "Global quieting of high-frequency seismic noise due to COVID-19 pandemic lockdown measures," Science (80-.). 369(6509), 1338–1343 (2020).

[6] D. E. McNamara and R. P. Buland, "Ambiente noise levels in the continental United States," Bull. Seismol. Soc. Am. 94(4), 1517–1527 (2004).

[7] N. Riahi and P. Gerstoft, "The seismic traffic footprint: Tracking trains, aircraft, and cars seismically," Geophys. Res. Lett. 42(8), 2674–2681 (2015).

[8] G. Ginaya, M. Ruki, and N. W. Wahyu Astuti, "Zero Dollar Tourists: Critical Analisys on Discourse of Chinese Market Segment in Bali Tourism," J. Kaji. Bali 9(1), 141–164 (2019).

[9] M. Arroyo-Solórzano, D. Castro-Rojas, F. Massin, L. Linkimer, I. Arroyo, and R. Yani, "COVID-19 lockdown effects on the seismic recordings in Central America," Solid Earth 12(10), 2127–2144 (2021).

[10] B. Grecu, F. Borleanu, A. Tiganescu, N. Poiata, R. Dinescu, and D. Tataru, "The effect of 2020 COVID-19 lockdown measures on seismic noise recorded in Romania," Solid Earth 12(10), 2351–2368 (2021).

[11] K. H. Chen, T. C. Yeh, Y. Chen, C. W. Johnson, C. H. Lin, Y. C. Lai, M. H. Shih, P. Guéguen, W. G. Huang, and B. S. Huang, "Characteristics and impact of environmental shaking in the Taipei metropolitan area," Sci. Rep. 12 (1)" (2022).

[12] D. N. Green, I. D. Bastow, B. Dashwood, and S. E. J. Nippress, "Characterizing broadband seismic noise in Central London," Seismol. Res. Lett. 88(1), 113–124 (2017).

[13] T.-K. Hong, J. Lee, G. Lee, J. Lee, and S. Park, "Correlation between ambient seismic noises and economic growth," Seismol. Res. Lett. 91(4), 2343–2354 (2020).

[14] H. Nimiya, T. Ikeda, and T. Tsuji, "Temporal changes in anthropogenic seismic noise levels associated with economic and leisure activities during the COVID-19 pandemic," Sci. Rep. 11(1) (2021).

[15] M. O. H. M. O. H. MYINT THU and S. Singh, "Study of the acoustic features and exposures of some typical construction noise sources in India," INTER-NOISE NOISE-CON Congr. Conf. Proc. 270, 7614–7620 (2024).

[16] A. L. Ponomarev, T. S. Ulanova, O. A. Molok, and A. A. Odegov, "Environmental Noise Measurement Technique and Evaluation of Contribution of a Large Industrial Enterprise to Noise Pollution in the Neighboring Residential Area," Public Heal. Life Environ. 2022(12), 59–65 (2022).

[17] B. Saadia and G. Fotopoulos, "Unsupervised clustering of ambient seismic noise in an urban environment," Comput. Geosci. 179 (2023).

[18] K. Sumaja, I. K. M. Satriyabawa, S. Maharani, and W. A. Mustika, "The Climate Comfort and Risk Assessment for Tourism in Bali, Indonesia," Springer Proc. Phys. 290, 545–553 (2023).

[19] P. D. Welch, "The use of fast Fourier transform for the estimation of power spectra: A method based on time averaging over short, modified periodograms," IEEE Trans. audio Electroacoust. 15(2), 70–73 (1967).

[20] R. E. Anthony, A. T. Ringler, D. C. Wilson, M. Bahavar, and K. D. Koper, "How processing methodologies can distort and bias power spectral density estimates of seismic background noise," Seismol. Res. Lett. 91(3), 1694–1706 (2020).

[21] J. R. Peterson, "Observations and modeling of seismic background noise" (1993).

[22] A. N. Besedina and T. A. Tubanov, "Microseisms as a tool for geophysical research. A review," J. Volcanol. Seismol. 17(2), 83–101 (2023).

[23] S. Bonnefoy-Claudet, F. Cotton, and P.-Y. Bard, "The nature of noise wavefield and its applications for site effects studies: A literature review," Earth-Science Rev. 79(3–4), 205–227 (2006).

[24] J. Díaz, M. Ruiz, P. S. Sánchez-Pastor, and P. Romero, "Urban Seismology: On the origin of earth vibrations within a city," Sci. Rep. 7(1) (2017).

[25] J. Clarke, L. Adam, K. van Wijk, and J. Sarout, "The influence of fluid type on elastic wave velocity and attenuation in volcanic rocks," J. Volcanol. Geotherm. Res. 403 (2020).

[26] D. G. Albert and S. N. Decato, "Acoustic and seismic ambient noise measurements in urban and rural areas," Appl. Acoust. 119, 135–143 (2017).

[27] V. K. Lemzikov and M. V Lemzikov, "Estimating the Attenuation of Seismic Wave Energy at Short Distances from Kizimen Volcano, Kamchatka," J. Volcanol. Seismol. 14(4), 211–219 (2020).

[28] C. Martínez-Arévalo, F. Bianco, J. M. Ibánez, and E. Del Pezzo, "Shallow seismic attenuation and shear-wave splitting in the short period range of Deception Island volcano (Antarctica)," J. Volcanol. Geotherm. Res. 128(1–3), 89–113 (2003).

[29] E. D. Pezzo, "Chapter 13 Seismic Wave Scattering in Volcanoes," Adv. Geophys. 50, 353–371 (2008).

[30] M. B. E. Mørk, "Diagenesis and quartz cement distribution of low-permeability Upper Triassic-Middle Jurassic reservoir sandstones, Longyearbyen CO2 lab well site in Svalbard,

Norway," Am. Assoc. Pet. Geol. Bull. 97(4), 577–596 (2013).
[31] Y. Xu, X. Yang, and L. Mei, "Reservoir Characteristics and Main Control Factors of Conglomerate Reservoir of El3 in the Northwest Steep Slope Zone of Weixinan Depression," Diqiu Kexue - Zhongguo Dizhi Daxue Xuebao/Earth Sci. - J. China Univ. Geosci. 45(5), 1706–1721 (2020).
[32] J. Yan, J. Fan, M. Wang, Z. Li, Q. Hu, and J. Chao, "Rock fabric and pore structure of the Shahejie sandy conglomerates from the Dongying depression in the Bohai Bay Basin, East China," Mar. Pet. Geol. 97, 624–638 (2018).
[33] M. M. Purbo-Hadiwidjoyo, H. Samodra, and T. C. Amin, "Geological map of the Bali sheet 1:250,000," Geological Research and Development Centre, Bandung, Indonesia. (1998).
[34] A. Chaaraoui, M. Chourak, J. A. Peláez, and S.-E. Cherif, "Seismic site effects investigation in the urban area of Nador (NE Morocco) using ambient noise measurements," Arab. J. Geosci. 14(18) (2021).
[35] A. K. Mundepi and A. Paul, "Estimation of site amplification at various litho-units in NW-Himalaya using horizontal to vertical ratio," J. Geol. Soc. India 70(4), 605–609 (2007).
[36] K. Wawrzyniak, "Frequency content of P and S waves in different lithologies from acoustic full waveforms," Near Surf. 2005 (2005).
[37] L. Gisselbrecht, B. Froment, P. Boué, and C. Gélis, "Insights into the conditions of application of noise-based spectral ratios in a highly industrialized area: a case study in the French Rhone Valley," Geophys. J. Int. 234(2), 985–997 (2023).
[38] T. V Efremova and Y. N. Goryachkin, "Anthropogenic Impact on the Lithodynamics of the Coastal Zone of the Southern and Western Black Sea Coast (Review)," Ecol. Saf. Coast. Shelf Zo. Sea (2), 5–29 (2021).
[39] J. Diaz, M. Schimmel, M. Ruiz, and R. Carbonell, "Seismometers Within Cities: A Tool to Connect Earth Sciences and Society," Front. Earth Sci. 8 (2020).